

NJC

Accepted Manuscript



This is an *Accepted Manuscript*, which has been through the Royal Society of Chemistry peer review process and has been accepted for publication.

Accepted Manuscripts are published online shortly after acceptance, before technical editing, formatting and proof reading. Using this free service, authors can make their results available to the community, in citable form, before we publish the edited article. We will replace this *Accepted Manuscript* with the edited and formatted *Advance Article* as soon as it is available.

You can find more information about *Accepted Manuscripts* in the [Information for Authors](#).

Please note that technical editing may introduce minor changes to the text and/or graphics, which may alter content. The journal's standard [Terms & Conditions](#) and the [Ethical guidelines](#) still apply. In no event shall the Royal Society of Chemistry be held responsible for any errors or omissions in this *Accepted Manuscript* or any consequences arising from the use of any information it contains.



Journal Name

COMMUNICATION

Nanoscale cobalt metal–organic framework as a catalyst for visible light-driven and electrocatalytic water oxidation

Received 00th January 20xx,
Accepted 00th January 20xx

Qian Xu,^a Hui Li,^a Fan Yue,^a Le Chi,^a Jide Wang*^a

DOI: 10.1039/x0xx00000x

www.rsc.org/

The Co-ZIF-67 metal–organic framework was investigated as a catalyst for visible light-driven and electrocatalytic water oxidation in basic and neutral media. Co-ZIF-67 exhibited efficient performance for visible light-driven water oxidation, with a turnover frequency of 0.035 s^{-1} . Co-ZIF-67 also maintained a stable current density after electrolysis for over 24 h, and it electrocatalyzed the oxygen evolution reaction within a wide pH range. DFT calculations suggest that the catalyst activates water molecules while the dissociated proton is received by nearby 2-methylimidazole ligands. This process permits Co-ZIF-67 to effectively catalyze the photocatalytic and electrocatalytic oxidation of water.

Since the 21st century, mankind has faced enormous energy pressure. Producing renewable clean energy has become a profound challenge. Solar energy is a clean energy source that contributes to sustainable energy development.¹ Scientists have long been interested in way to harvest solar energy efficiently. Plants can convert solar energy into chemical energy by photosynthesis, via a novel conversion pathway. Focused research efforts have been made to develop visible abiological water splitting system. However, water oxidation is still considered the most challenging step in the water splitting process because it is a more complex chemical reaction than proton reduction and provides a total of four electrons per molecule, thereby leading to O₂ formation ($2\text{H}_2\text{O} \rightarrow \text{O}_2 + 4\text{H}^+ + 4\text{e}^-$).² This oxygen evolution reaction (OER) is one of the most important naturally occurring processes in plant photosystem II (PSII) to provide electrons and protons, which are used by ATP synthase to generate ATP and to reduce CO₂ into carbohydrates while releasing oxygen gas into the atmosphere. Moreover, artificial photosynthetic water oxidation may contribute to the effective utilization the sunlight as an alternative energy source. In this regard, a considerable number of studies have

investigated artificial water oxidation catalysts (WOCs).³ Among these catalysts, cobalt-based compounds and oxides, such as the polyoxometalate cobalt (II) complex,^{4–11} mononuclear cobalt (II) complex,^{12–15} bio-inspired organic cobalt (II) phosphonates,^{16–18} and cobalt (II) oxide,^{19, 20} exhibit efficient performance for water oxidation.

Metal–organic frameworks (MOFs) with a large specific surface area and a special frame structure are extensively applied in gas storage,²¹ sensors,^{22, 23} and catalysis.^{24, 25} Lin et al.²⁶ first reported the incorporation of Ir, Re, and Ru complexes into the UiO framework; their group demonstrated that porous MOFs doped with a metal complex derivative are effective catalysts for water oxidation. Wang et al.²⁷ also introduced a novel type of heterogeneous WOCs by the assembly of cobalt ions and benzimidazole ligands into crystalline microporous MOFs (Co-ZIF-9). This catalyst displayed exclusive oxygen evolution from water when coated on a fluorine-doped tin oxide (FTO) glass side, to generate 8 μmol of dioxygen within 3 h, with a turnover frequency (TOF) of $1.76 \times 10^{-3}\text{ s}^{-1}$. Zeolitic imidazolate frameworks (ZIFs) are a subclass of MOFs with a tetrahedral network structure and a large surface area.²⁸ ZIFs have been extensively used in hydrogen storage²⁹ and CO₂ capture/conversion^{30, 31}, because of their outstanding characteristics. However, to the best of our knowledge, the application of unmodified ZIFs in the photocatalytic oxidation of water has not yet been reported. In this study, unmodified cobalt-based ZIFs (Co-ZIF-67) were used as a heterogeneous catalyst with [Ru(bpy)₃]²⁺ (bpy = 2,2'-bipyridine) as the photosensitizer (PS) and Na₂S₂O₈ as the sacrificial electron acceptor. This catalyst was significantly effective for water oxidation. Finally, we demonstrated that Co-ZIF-67 electrocatalysts are highly stable.

Photocatalytic reaction mixtures with different catalyst amounts, buffer types, pH values, and photosensitizers were systemically investigated to determine the optimal reaction conditions (Figs. S4–S7 ESI†). The amount of evolved O₂ increased as the Na₂S₂O₈ concentration increased to 40 mM. The maximum amount of O₂ formation was 117.2 μmol was achieved (Fig. 1). The reaction rate was high, and the TOF of O₂ evolution was 0.035 s^{-1} . However, the catalytic activity is observed to become decreased when the amount of Co-ZIF-67 was increased to 1.0 mg. The pH meter was used detect pH of after the catalytic reaction, which was

^aMinistry Key Laboratory of oil and Gas Fine Chemical, College of Chemistry and Chemical Engineering Xinjiang University, Shengli Road, Urumqi 830046, China. E-mail: awangjd@126.com

†Electronic Supplementary Information (ESI) available. See DOI: 10.1039/x0xx00000x

decreased from 9.00 to 5.53. In the acidic conditions, there are which contribute to accumulation of $[\text{Ru}(\text{bpy})_3]^{3+}$. The process of eqn (1) became the rate-limiting step ($4[\text{Ru}(\text{bpy})_3]^{3+} + 2\text{H}_2\text{O} \rightarrow 4[\text{Ru}(\text{bpy})_3]^{2+} + \text{O}_2 + 4\text{H}^+$ (Equation 1)). The existence of build-up $[\text{Ru}(\text{bpy})_3]^{3+}$ was proved by its characteristic absorbance at 683 nm by UV-vis (Fig. S14 and S15 ESI[†]). Based on the above experimental, we hypothesized that with the increase of catalyst amount, the reaction environment has changed dramatically that result of low rate and similar amount of O_2 .

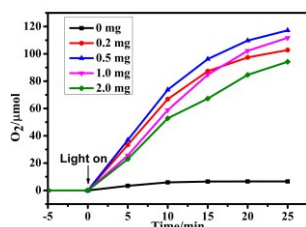


Fig. 1 Kinetics of O_2 evolution of the photocatalytic system with different amounts of Co-ZIF-67 (0 mg, black; 0.2 mg, red; 0.5 mg, blue; 1.0 mg, pink; 2.0 mg, green). Conditions: Xe lamp ($\lambda \geq 420$ nm, $26.4 \text{ mW}\cdot\text{cm}^{-2}$); 1.0 mM $[\text{Ru}(\text{bpy})_3](\text{ClO}_4)_2$, 40.0 mM $\text{Na}_2\text{S}_2\text{O}_8$, and 80 mM sodium borate buffer (initial pH, 9.0); total reaction volume: 10 mL.

Here, through simply altering the solvent and reaction temperature, we obtained Co-ZIF-67 with different sizes (Fig. S2 ESI[†]). The effect of different sizes on the photocatalytic performance was studied. As shown in Fig. S3 ESI[†]. As the size of the Co-ZIF-67 decreases, the catalysts show an increased photocatalytic activity. That mainly due to the smaller structure could provide more active and convenient catalytic centers and thus promote a faster mass and electron transfer process.

The Co-ZIF-67 catalyst was recovered and reused for subsequent photocatalytic reactions after the first run. The catalyst was still highly active in the subsequent cycles (Fig. S8 ESI[†]). When suspended in fresh solution, the catalyst induced oxygen evolution under light irradiation, although with a lower TOF of 0.020 s^{-1} . The decreased catalytic activity was possibly caused by the loss of catalytic particles during the recovery process. The reduced catalytic activity in the second cycle has also been reported for recovered spinel oxide WOCs.^{32, 33}

Secondary WOC species formed through PS and catalyst decomposition have recently become a very critical issue for researchers. A series of measurements were obtained. First, dynamic light scattering (DLS) was conducted to detect the reaction solution after illumination. Any nanoparticle formation below 1000 nm was identified (Fig. S9 ESI[†]). Second, contrast test to exclude RuO_2 as a catalytically active species was performed by replacing Co-ZIF-67 with amounts of Ru-containing references (RuO_2 and $\text{RuCl}_3 \cdot x\text{H}_2\text{O}$). These experiments verified the absence of oxygen evolution comparable to Co-ZIF-67, strongly revealing that PS decomposition products did not act as the active species under standard conditions (Fig. S10 ESI[†]). Thirdly, the Co-ZIF-67 leaching was analyzed by inductive coupled plasma emission spectrometer (ICP). Aging 0.5 mg of Co-ZIF-67 in 80 mM pH=9.0 sodium borate buffer for 3 h, yielded a concentration of cobalt at 0.014 mM remaining in the solution. The ICP analysis results indicated that less than 6% of Co-ZIF-67 could have leached to release Co^{2+} in the

borate buffer. Finally, the supernatant post-catalytic solution was recovered by centrifugation and then analyzed by liquid chromatography-mass spectrometry (LC-MS). The species observed in the mass spectra were $[\text{Ru}(\text{bpy})_3]^{2+}$ (m/z : 285.25) and $[\text{Ru}(\text{py})_3](\text{ClO}_4)_2^+$ (m/z : 536.06) (Fig. S17 ESI[†]). At m/z between 100–1000, no Co-ZIF-67, free 2-methylimidazole or other cobalt species were found.

The X-ray photoelectron spectroscopy (XPS) was used to analyze the surface conditions of Co-ZIF-67 before and after the photocatalytic reaction. The energy regions of Co 2p and N 1s in the particles are shown in Figs. 2a and 2b, respectively. The similar ratios of peak strength between the Co 2p main peak and the satellite peak for both samples showed that the surface conditions remain unchanged even after the photocatalytic water oxidation under highly oxidizing conditions.³⁴ This result was further confirmed by the N 1s peak for Co-ZIF-67 before and after the reaction. The Co-ZIF-67 catalysts were tested before and after the reaction by powder XRD, and no obvious variation was observed (Fig. S18 ESI[†]). Co-ZIF-67 is highly robust even during the photocatalytic water oxidation.³⁵

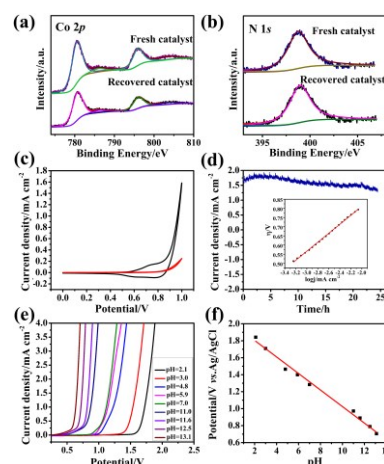


Fig. 2 XPS of Co-ZIF-67 catalyst particles before and after a catalytic cycle in the energy regions of (a) Co 2p and (b) N 1s. The binding energy of each element was corrected by the C 1s peak (284.8 eV). (c) Cyclic voltammograms of the FTO glass background (red line) and 0.25 $\text{mg}\cdot\text{cm}^{-2}$ of the Co-ZIF-67/FTO electrode (black line) in 80 mM sodium borate buffer (pH=9.0). (d) Dependence of current density on time over the Co-ZIF-67/FTO electrode in 0.1 M phosphate buffer (pH=7.0). Inset: Tafel plot of the Co-ZIF-67/FTO electrode. (e) pH dependence of CVs measured at different pH values (2.1–13.1) over the Co-ZIF-67/FTO electrode. (f) pH dependence of steady-state electrode potential at constant current density ($I_{\text{anodic}}=4.0 \text{ mA}\cdot\text{cm}^{-2}$) over the Co-ZIF-67/FTO electrode. The Ag/AgCl electrode was used as reference.

The electrochemical properties of Co-ZIF-67 were investigated (Figs. 2c–2f). The CV of Co-ZIF-67 showed a small oxidation peak at 0.75 V (vs. Ag/AgCl), which is considered $\text{Co}^{\text{III/II}}$ oxidation, followed by a catalytic oxidation wave (Fig. 2c). The onset of the catalytic wave attributed to water oxidation is observed at approximately 0.6 V (vs. Ag/AgCl). By contrast, only the minimum current was obtained in the same buffered solution without Co-ZIF-67. Clearly, Co-ZIF-67 can catalyze the water oxidation reaction.

Furthermore, pristine Co-ZIF-67 was transferred onto the FTO glass electrode for a long-term test. A stable current was observed after 5 h and 24 h of operation in the acidic and neutral solution, respectively (Fig. S23 ESI[†] and 2d). The pH dependence test of the OER showed that the overpotential for OER decreases with increasing pH (Fig. 2e). At a constant current density ($4.0 \text{ mA}\cdot\text{cm}^{-2}$), the potential was measured *versus* the pH to reveal that a constant decrease from pH=13.1 to pH=2.1 with a slope of -97 mV per pH (Fig. 2f). This value is close to -93 mV per pH reported in the literature.²⁷ Therefore, Co-ZIF-67 is stable and effective in a wide pH range of basic. Additionally, the LSV curves were recorded after different potential cycles in the basic and acidic solution (Fig. S19 and S24 ESI[†]). No matter in the basic and acidic conditions, Co-ZIF-67 afforded almost the same current density–potential curves as the initial reading. XPS measurements of the energy region of Co2p and N1s were performed after the CV scans (Fig. S20 ESI[†]), clearly revealing that Co-ZIF-67 exhibits high stability as a water electrolysis catalyst.

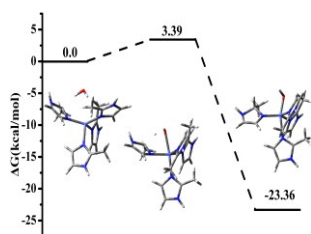
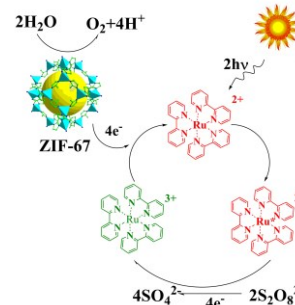


Fig. 3 DFT-calculated energetic and geometries of the initial dehydrogenation of the water molecule. Atoms: H (white), C (gray), N (dark blue), Co (light blue), O (red).

DFT calculation results show that Co-ZIF-67 can catalyze water splitting via abstraction of hydrogen atoms in water. The key step in this process is the initial dehydrogenation of H_2O molecules during oxidation. The optimization of the initial, transition, and final states of the water molecular dissociation reaction is shown in Fig. 3. In the initial state, water molecules are trapped by the Co-ZIF-67 catalyst, with the hydrogen atom (H) pointing to the carbon atom (C) of Co-ZIF-67 ($d_{\text{C-H}}=1.86 \text{ \AA}$). In the transition state, H dissociates from O, with a distance of approximately 1.15 \AA . By contrast, in the initial state, H is close to C ($d_{\text{C-H}}=1.53 \text{ \AA}$), with a distance of approximately 1.02 \AA . However, the activation energy barrier is low ($3.38 \text{ kcal}\cdot\text{mol}^{-1}$), which indicates that the reaction tends to occur at low temperatures. This step is exothermic and has a reaction heat of $-23.36 \text{ kcal}\cdot\text{mol}^{-1}$. In the final state, the length of the C–H bond is 1.12 \AA . The completely formed OH species is adsorbed onto Co atoms, with a Co–O bond length of 1.96 \AA . The formed OH species may continue to fracture. Related research on this topic will be conducted in the future. The DFT calculations show that the Co-ZIF-67 catalyst with C ligands contributes to the direct abstraction of H atoms via substrate water binding to the Co active site. This finding indicates that 2-methylimidazole functions as a proton acceptor during catalysis to induce proton-coupled electron transfer during water oxidation.

Scheme 1 shows the proposed mechanism of visible light-driven water oxidation. $[\text{Ru}^{\text{II}}(\text{bpy})_3]^{2+}$ ions are generated from $[\text{Ru}^{\text{II}}(\text{bpy})_3]^{2+}$ absorption and the consumption two photons under

illumination. The $[\text{Ru}^{\text{II}}(\text{bpy})_3]^{2+}$ enters the visible light-accessible metal-to-ligand charge-transfer excited state via $\text{S}_2\text{O}_8^{2-}$ quenching, thereby generating four $[\text{Ru}^{\text{III}}(\text{bpy})_3]^{3+}$ complexes two SO_4^{2-} , and two $\text{SO}_4^{\cdot -}$. The $[\text{Ru}^{\text{III}}(\text{bpy})_3]^{3+}$ and $\text{SO}_4^{\cdot -}$ [$\text{E}(\text{SO}_4^{\cdot -}/\text{SO}_4^{2-})\approx 2.4 \text{ V}$]³⁶ are both strong oxidants that sequentially oxidize Co-ZIF-67, which in turn oxidizes H_2O to O_2 and regenerates $[\text{Ru}^{\text{II}}(\text{bpy})_3]^{2+}$.



Scheme 1 Principal processes of O_2 evolution from a light-driven water oxidation system.

In summary, we report the use of nanoscale cobalt MOFs (Co-ZIF-67) as an efficient heterogeneous catalyst for water oxidation. The catalytic property of Co-ZIF-67 was evaluated by its photoreaction and electroreaction. The results revealed that Co-ZIF-67 is an effective catalyst under visible light irradiation and presents a TOF of 0.035 s^{-1} at pH=9.0, with $[\text{Ru}(\text{bpy})_3](\text{ClO}_4)_2$ as photosensitizer and $\text{Na}_2\text{S}_2\text{O}_8$ as the sacrificial electron acceptor. Co-ZIF-67 has been shown to electrocatalyze the OER over a wide pH range. Co-ZIF-67 contains abundant cobalt combined with 2-methylimidazole ligands as proton transfer and redox mediators to facilitate the photochemical and electrochemical catalysis of water oxidation. Intensive research on MOF-based WOCs by framework engineering would be widespread in the future.

Experimental

300 nm of Co-ZIF-67 was synthesized according to reference.³⁷ 1.436 g of $\text{Co}(\text{NO}_3)_2\cdot 6\text{H}_2\text{O}$ and 3.244 g of 2-methylimidazole were each dissolved in 100 mL methanol at 25°C . The former salt solution was poured into the latter ligand solution under vigorous stirring. The mixture was stirred for 30 min and then kept for 24 h. The solid product was separated by centrifugation and washed with methanol three times, followed by vacuum during at 70°C for 8 h.

Acknowledgements

We acknowledge funding support from the Nature Science Foundation of China (NSFC) (no. 21261022, 21162027).

Notes and references

1. L. Hammarstrom and S. Hammes-Schiffer, *Acc.Chem.Res.*, 2009, 42, 1859–1860.
2. Q. Yin, J. M. Tan, C. Besson, Y. V. Geletii, D. G. Musaev, A. E. Kuznetsov, Z. Luo, K. I. Hardcastle and C. L. Hill, *Science*, 2010, 328, 342–345.
3. J. Barber, *Chemical Society Reviews*, 2009, 38, 185–196.
4. G. La Ganga and F. Puntoriero, *Pure and Applied Chemistry*, 2015.

5. X. B. Han, Z. M. Zhang, T. Zhang, Y. G. Li, W. Lin, W. You, Z. M. Su and E. B. Wang, *Journal of the American Chemical Society*, 2014, 136, 5359-5366.
6. P.-E. Car, M. Guttentag, K. K. Baldrige, R. Alberto and G. R. Patzke, *Green Chemistry*, 2012, 14, 1680.
7. Z. Huang, Z. Luo, Y. V. Geletii, J. W. Vickers, Q. Yin, D. Wu, Y. Hou, Y. Ding, J. Song, D. G. Musaev, C. L. Hill and T. Lian, *Journal of the American Chemical Society*, 2011, 133, 2068-2071.
8. R. Schiwon, K. Klingan, H. Dau and C. Limberg, *Chemical communications*, 2014, 50, 100-102.
9. N. Anwar, A. Sartorel, M. Yaqub, K. Wearen, F. Laffir, G. Armstrong, C. Dickinson, M. Bonchio and T. McCormac, *ACS applied materials & interfaces*, 2014, 6, 8022-8031.
10. F. Song, Y. Ding, B. Ma, C. Wang, Q. Wang, X. Du, S. Fu and J. Song, *Energy & Environmental Science*, 2013, 6, 1170.
11. J. J. Stracke and R. G. Finke, *ACS Catalysis*, 2014, 4, 909-933.
12. S. Fu, Y. Liu, Y. Ding, X. Du, F. Song, R. Xiang and B. Ma, *Chemical communications*, 2014, 50, 2167-2169.
13. H. Wang, Y. Lu, E. Mijangos and A. Thapper, *Chinese Journal of Chemistry*, 2014, 32, 467-473.
14. R. Xiang, Y. Ding and J. Zhao, *Chemistry—An Asian Journal*, 2014, 9, 3228-3237.
15. D. Hong, J. Jung, J. Park, Y. Yamada, T. Suenobu, Y.-M. Lee, W. Nam and S. Fukuzumi, *Energy & Environmental Science*, 2012, 5, 7606-7616.
16. D. Shevchenko, M. F. Anderlund, A. Thapper and S. Styring, *Energy & Environmental Science*, 2011, 4, 1284-1287.
17. K. Y. Ju, S. Lee, J. Pyo, J. Choo and J. K. Lee, *Small*, 2015, 11, 84-89.
18. T. Zhou, D. Wang, S. C.-K. Goh, J. Hong, J. Han, J. Mao and R. Xu, *Energy & Environmental Science*, 2015.
19. S. Zhao, C. Li, J. Liu, N. Liu, S. Qiao, Y. Han, H. Huang, Y. Liu and Z. Kang, *Carbon*, 2015, 92, 64-73.
20. N. Shi, W. Cheng, H. Zhou, T. Fan and M. Niederberger, *Chemical communications*, 2015, 51, 1338-1340.
21. L. J. Murray, M. Dincă and J. R. Long, *Chemical Society Reviews*, 2009, 38, 1294-1314.
22. M. D. Allendorf, R. J. T. Houk, L. Andruszkiewicz, A. A. Talin, J. Pikaesky, A. Choudhury, K. A. Gall and P. J. Hesketh, *Journal of American Chemical Society*, 2008, 130, 14404-14405.
23. A. Lan, K. Li, H. Wu, D. H. Olson, T. J. Emge, W. Ki, M. Hong and J. Li, *Angewandte Chemie International Edition*, 2009, 48, 2334-2338.
24. L. Ma, C. Abney and W. Lin, *Chemical Society Reviews*, 2009, 38, 1248-1256.
25. F. Song, C. Wang, J. M. Falkowski, L. Ma and W. Lin, *Journal of the American Chemical Society*, 2010, 132, 15390-15398.
26. C. Wang, Z. Xie, K. E. deKrafft and W. Lin, *Journal of the American Chemical Society*, 2011, 133, 13445-13454.
27. S. Wang, Y. Hou, S. Lin and X. Wang, *Nanoscale*, 2014, 6, 9930-9934.
28. R. Banerjee, A. Phan, B. Wang, C. Knobler, H. Furukawa, M. O'Keefe and O. M. Yaghi, *Science*, 2008, 319, 939-943.
29. H. Wu, W. Zhou and T. Yildirim, *Journal of the American Chemical Society*, 2007, 129, 5314-5315.
30. T. Wang and N. Jiao, *Accounts of chemical research*, 2014, 47, 1137-1145.
31. S. Wang, W. Yao, J. Lin, Z. Ding and X. Wang, *Angewandte Chemie International Edition*, 2014, 53, 1167-1167.
32. M. Grzelczak, J. Zhang, J. Pfrommer, J. r. Hartmann, M. Driess, M. Antonietti and X. Wang, *ACS Catalysis*, 2013, 3, 383-388.
33. H. Liu and G. R. Patzke, *Chemistry—An Asian Journal*, 2014, 9, 2249-2259.
34. X. Du, Y. Ding, R. Xiang and X. Xiang, *Physical Chemistry Chemical Physics*, 2015, 17, 10648-10655.
35. Y. Maenaka, T. Suenobu and S. Fukuzumi, *Journal of the American Chemical Society*, 2012, 134, 9417-9427.
36. Y. Yamada, K. Yano, D. Hong and S. Fukuzumi, *Physical Chemistry Chemical Physics*, 2012, 14, 5753-5760.
37. W. Xia, J. Zhu, W. Guo, L. An, D. Xia and R. Zou, *Journal of Materials Chemistry A*, 2014, 2, 11606.

The Co-ZIF-67 are proposed as efficient water oxidation catalysts under visible light-driven.

